

Nonuniqueness of fluctuating momentum in coarse-grained systemsM. Reza Parsa,^{1,*} Changho Kim^{1,†} and Alexander J. Wagner^{2,‡}¹*Department of Applied Mathematics, University of California, Merced, California 95343, USA*²*Department of Physics, North Dakota State University, Fargo, North Dakota 58108, USA*

(Received 18 December 2020; revised 26 May 2021; accepted 7 June 2021; published 9 July 2021)

Coarse-grained descriptions of microscopic systems often require a mesoscopic definition of momentum. The question arises as to the uniqueness of such a momentum definition at a particular coarse-graining scale. We show here that particularly the fluctuating properties of common definitions of momentum in coarse-grained methods like lattice gas and lattice Boltzmann do not agree with a fundamental definition of momentum. In the case of lattice gases, the definition of momentum will even disagree in the limit of large wavelength. For short times we derive analytical representations for the distribution of different momentum measures and thereby give a full account of these differences.

DOI: [10.1103/PhysRevE.104.015304](https://doi.org/10.1103/PhysRevE.104.015304)**I. INTRODUCTION**

The definition of coarse-grained quantities for a mesoscopic simulation method can be subtle [1]. In this article we investigate the connection between the atomistic definition of momentum and the lattice gas (or lattice Boltzmann) definition of momentum [2], in particular, the definition of the fluctuating component of the momentum [3]. It is usually assumed that momentum is a uniquely defined quantity. For coarse-grained descriptions, however, this is not necessarily the case, since space and time averages impact the definition of fluctuating components of the momentum.

We show here that different definitions of microscopic momentum differ significantly. In particular the definition of the fluctuating momentum through a lattice gas deviates significantly from a molecular definition of momentum. We show that momentum definitions for a lattice gas differ from molecular dynamics based definitions not only at the scale of the lattice, but even in the hydrodynamic limit, i.e., for large wavelength. This is particularly true for short timescales, where the motion of particles is approximately ballistic. At a larger level of coarse-graining, where significant correlations are present, MD and LG definitions appear to converge.

These insights are important when considering the correct implementation of fluctuations in mesoscopic methods like fluctuating lattice Boltzmann [4–6], lattice gas [7], dissipative particle dynamics [8,9], or stochastic rotation dynamics [10–12]. We focus here on lattice gas and lattice Boltzmann implementations, and we will use the MDLG procedure to directly map between MD and lattice gas or lattice Boltzmann. In Sec. II we will briefly introduce lattice gases and the MDLG mapping.

II. LATTICE GAS AND MDLG

The key idea of the MDLG procedure is to map an MD simulation onto a discrete particle evolution on a lattice that has the same formal representation as a lattice gas. To explain this procedure we briefly introduce boolean as well as integer lattice gas models and explain in which key aspects they differ from the MDLG coarse-graining onto a lattice gas. Boolean lattice gases were originally developed as minimal models for statistical mechanics. To simulate hydrodynamic systems, the lattice collisions that conserved both particle number and lattice gas momentum were chosen. It was the key accomplishment by Frisch, Hasslacher and Pomeau [2] and Wolfram [13] to select a lattice with sufficient rotational symmetry to recover the Navier-Stokes equations, albeit with some constants that contain unwanted density and velocity dependence. But for practical purposes it was possible to use this method for perfectly adequate fluid simulations, as long as the density variations were not too great. The inherent fluctuations of the lattice gas method were a great advantage for some applications [14,15]. It was also of interest how the lattice gas density fluctuations can be related to fundamental molecular theory [3,16] or mode coupling theory [17]. However, these fluctuations were not universally helpful, and averaged (i.e., deterministic) lattice Boltzmann methods were developed [18]. By choosing a different equilibrium distribution it was also possible to remove the density and velocity dependence in the Navier-Stokes equations [19,20]. This significant advantage then spurred the development of lattice Boltzmann methods that also included fluctuations [5,21,22]. It was only recently realized that it is possible to develop a lattice gas method that has the same hydrodynamic limit as an entropic lattice Boltzmann method. This is achieved by allowing for integer occupation numbers, rather than only boolean occupation numbers [23]. The Boltzmann limit of this lattice gas was shown to be a known entropic lattice Boltzmann method [24].

To directly link an MD simulation to a lattice gas we utilize the Molecular Dynamics Lattice Gas procedure [25]. It

*mparsa@ucmerced.edu

†ckim103@ucmerced.edu

‡alexander.wagner@ndsu.edu; www.ndsu.edu/pubweb/~carswag

identifies the lattice gas occupation numbers $n_i(x, t)$ as the number of particles that move from lattice site $\xi - c_i$ at time $t - \Delta t$ to lattice site ξ at time t . Here the c_i are lattice displacements, and they are the set of all distances between lattice sites. For a cubic lattice with lattice spacing Δx we get

$$c_{i,\alpha} \in \{0, \pm 1, \pm 2, \dots\} \frac{\Delta x}{\Delta t} \quad (1)$$

for each Cartesian direction indicated by the Greek symbol α . The c_i are typically referred to as the “velocity set” in a lattice gas or lattice Boltzmann context. The only difference here is that the velocity set in principle contains all possible lattice displacements instead of being restricted a priori to a small set of lattice displacements. The effective size of the velocity set then emerges by considering only the lattice displacements for which there are actually particles experiencing them. First we define a function that determines if the coordinates lie inside a lattice site denominated by ξ as

$$\Delta_\xi(x) = \begin{cases} 1 & \text{if } x \in \xi, \\ 0 & \text{otherwise.} \end{cases} \quad (2)$$

We can then express the occupation numbers mathematically as

$$n_i(\xi, t) = \sum_n \Delta_{\xi-c_i}[x_n(t - \Delta t)] \Delta_\xi[x_n(t)], \quad (3)$$

where $x_n(t)$ is the position of the n th particle in the MD simulation at time t . Here the n_i take on integer values, and these n_i obey an evolution equation that is formally similar to the standard lattice gas evolution equation:

$$n_i(\xi + c_i, t + \Delta t) = n_i(\xi, t) + \Xi_i. \quad (4)$$

However, it is important to note that in the MDLG context the definition of the n_i is the fundamental quantity given by Eq. (3), and the collision operator is determined by the n_i through

$$\Xi_i = n_i(\xi + c_i, t + \Delta t) - n_i(\xi, t). \quad (5)$$

This collision operator is therefore a fluctuating quantity which is fully defined through the underlying MD simulation. The collision operator conserves mass but not momentum. The standard lattice gas definition for the mass and momentum fields are

$$\rho^{\text{LG}}(\xi, t) = \sum_i n_i(\xi, t), \quad (6)$$

$$j^{\text{LG}}(\xi, t) = \sum_i c_i n_i(\xi, t) \quad (7)$$

and are also applied here. Note that this definition uses our convention that the particles have a unit mass $m = 1$. The average occupation numbers define an equilibrium distribution function

$$f_i^{\text{eq}} = \langle n_i \rangle. \quad (8)$$

This equilibrium distribution function is in good agreement of the standard lattice Boltzmann equilibrium distributions only for a very specific choice of lattice spacing Δx and timestep size Δt . To achieve this the lattice spacing Δt is determined

by the constraint

$$a^2 = \frac{\langle \delta x^2 \rangle}{d \Delta x^2} \approx \frac{2}{11}, \quad (9)$$

where $\delta x = x(t + \Delta t) - x(t)$ is the displacement of a particle during a time interval Δt , $\langle \delta x^2 \rangle$ is the mean-squared displacement and d is the number of dimensions. This value of a^2 was chosen over $1/6$, which was used in the original publication [25], for purely historical reasons. The tiny difference between the two values for the current study is irrelevant. For this choice of $a^2 = 2/11$ we only have lattice velocities $c_{ix} \in \{-1, 0, 1\} \Delta x / \Delta t$ with appreciable probabilities [25].

We know that the underlying momentum in the MD simulation is conserved and that the lattice gas momentum, which only takes on discrete values, cannot be identical to the MD momentum. We therefore want to examine the similarities and differences in these two definitions of momentum.

III. DEFINITIONS FOR MOMENTUM

For our MD simulations we consider classical particles where the n th particle has a position $x_n(t)$ and a velocity $v_n(t) = dx_n(t)/dt$. The density is then simply given by

$$\rho(x, t) = \sum_n \delta[x - x_n(t)], \quad (10)$$

and the local momentum can be defined as

$$j(x, t) = \sum_n v_n(t) \delta[x - x_n(t)]. \quad (11)$$

To recover continuous density and momentum fields sometimes the Dirac δ function is replaced by a function with a finite base [26,27], but we do not consider these approaches here. We focus on mesoscale simulation methods that coarse-grain these fields onto a regular lattice (often a square or cubic lattice) with a lattice size of Δx . We can then define the lattice based definition ρ and j as

$$\rho(\xi, t) = \sum_n \Delta_\xi[x_n(t)], \quad (12)$$

$$j(\xi, t) = \sum_n v_n(t) \Delta_\xi[x_n(t)]. \quad (13)$$

This is the most straightforward projection of the conserved quantities of mass and momentum onto a lattice.

The definition of the lattice density ρ^{LG} of Eq. (6) is identical to the definition in the MD context Eq. (12)

$$\rho(\xi, t) = \rho^{\text{LG}}(\xi, t). \quad (14)$$

As mentioned above the momentum j differs from the lattice gas definition j^{LG} . In the previous publication [25] it was shown that while the instantaneous values of the current j and j^{LG} cannot be identical, the expectation values in the sense of a nonequilibrium ensemble average are the same:

$$\langle j(\xi, t) \rangle_{\text{neq}} = \langle j^{\text{LG}}(\xi, t) \rangle_{\text{neq}} \quad (15)$$

where $\langle \dots \rangle_{\text{neq}}$ denotes a nonequilibrium ensemble average. This has to be the case simply because mass is rigorously conserved both in MD and LG, the definition of mass is identical, and therefore the expectation value of the mass current also has to agree.

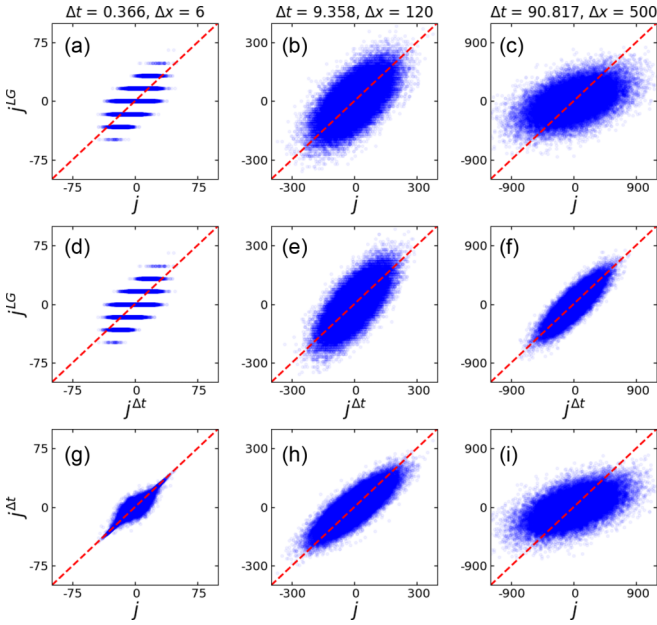


FIG. 1. Scatter plots for the correlations of three different momenta considered in this paper for three different time-steps Δt .

It is therefore interesting to examine how well the two nonaveraged definitions of the mass current are correlated. To examine the momentum definition we performed equilibrium MD simulations of a two dimensional Lennard-Jones (LJ) fluid given by the interparticle potential

$$V(x) = 4\epsilon \left[\left(\frac{\sigma}{x} \right)^{12} - \left(\frac{\sigma}{x} \right)^6 \right]. \quad (16)$$

For simplicity, we assumed the mass of one particle, m , equals one and the unit of time is scaled by $\tau = (m\sigma^2/\epsilon)^{1/2}$. We performed our MD simulations using the LAMMPS package [28]. The particles are contained in square box with the length of $L = 3000\sigma$ with periodic boundary conditions. Uniform configurations of $N = 90\,000$ particles with the kinetic energy corresponding to 50 in the LJ units were generated as an initial configuration. We ran our simulation with a time step of 0.001τ . The first 10 000 000 iterations were discarded and then measurements were performed for additional 10 000 000 timesteps. We saved data for specific Δx using a time-step that gave $a^2 = 2/11$ from Eq. (9). Furthermore, we used ADIOS2 package [29] along with MD simulations to reduce the time required for reading and analyzing data. For data presented in this paper we used a range of lattice size from 6σ to 500σ which led to different numbers of lattice points for our fixed simulation box.

In Fig. 1 the scatter plot shows the correlation of three different momentum definitions for three different timesteps Δt . The third definition will be given below, see Eq. (21). For j and j^{LG} we can see the correlation in Figs. 1(a)–1(c) for three different time-steps. The two measures j and j^{LG} are indeed not identical, which would be represented by blue points lying entirely on the red diagonal. Instead we observe noticeable scatter. Interestingly there is not only scatter, but the average does not even follow the identity, indicating that the widths of the momentum distributions for the two measures are

different. Which distribution is wider does depend on the time discretization. One further feature that immediately stands out is the strong discretization of j^{LG} for the shortest timestep. In this case there are on average only $\langle n \rangle = N\Delta x^2/L^2 = 0.36$ particles in each lattice site. We can use f_i^{eq} of Eq. (8) to define the combined occupation density for positive velocities as

$$f^+ = \sum_{i:c_{ix}>0} f_i^{\text{eq}}, \quad (17)$$

where the sum is only taking over those indices for which the lattice velocity has a positive x component. Similarly we can define f^- as the sum of all f_i^{eq} where the $c_{ix} < 0$. We also define the average number of particles on each lattice site as

$$\rho^{\text{eq}} = \sum_i f_i^{\text{eq}} = \frac{N\Delta x^2}{L^2}. \quad (18)$$

We can now ask which distribution of particles is expected for lattice momentum $l\Delta x/\Delta t$. If the particles can be considered independent, then the probability that a specific lattice site has the momentum $l\Delta x/\Delta t$ is equivalent to a standard combinatorial problem: given N particles that are to be distributed into three containers. The first container corresponds to a lattice velocity with $c_{ix} = +\Delta x/\Delta t$ at lattice site ξ , the second container corresponds to a lattice velocity with $c_{ix} = -\Delta x/\Delta t$ at the same site [the only values entering Eq. (7)], and the last one is the rest of the lattice. This gives the probability of

$$\begin{aligned} P(j_x^{\text{LG}} \equiv l\Delta x/\Delta t) &= \sum_k \frac{N!}{(N-2k-l)!k!(k+l)!} \\ &\times \left(1 - \frac{f^+ + f^-}{\rho^{\text{eq}}N_\xi} \right)^{N-2k-l} \left(\frac{f^+}{\rho^{\text{eq}}N_\xi} \right)^{k+l} \left(\frac{f^-}{\rho^{\text{eq}}N_\xi} \right)^k \end{aligned} \quad (19)$$

to find a total momentum of $l\Delta x/\Delta t$ where N_ξ is the number of lattice sites and we sum over all combinations that have a total momentum of $l\Delta x/\Delta t$, i.e., having k particles with lattice velocity $c_{ix} = -\Delta x/\Delta t$ and $k+l$ particles with lattice velocity $c_{ix} = +\Delta x/\Delta t$. Here we have approximately $f^- \approx \rho^{\text{eq}}/6$, $f^0 \approx 2\rho^{\text{eq}}/3$, and $f^+ \approx \rho^{\text{eq}}/6$ where f^0 is defined similar to the definition in Eq. (17) for particles with no x momentum. The number of lattice points is $N_\xi = 250\,000$. In Fig. 1 we show the values for momenta for 10 iterations. The expected number of points in the scatter plot with momentum $4\Delta x/\Delta t$ is then $10N_\xi P(j^{\text{LG}} \equiv 4\Delta x/\Delta t) \approx 1.198$. The expected number of samples with lattice momentum of 5 is 0.014. This is in good agreement with seeing two instances of lattice momentum of 4 (as well as none with a lattice momentum of -4), and no instance with a larger absolute lattice momentum. An alternative derivation that does not make the assumption of having only three velocities in any one direction is shown in Sec. IV C.

This explains why one distribution is discrete while the other is continuous. It does not, however, explain why the momenta are not distributed with the same second moment. To understand this better, we first observe that the momentum distribution j only depends on the instantaneous velocity of

the particles, where as j^{LG} depends on the displacement of the particles during the time interval Δt . We can therefore define an in-between measure consisting of the averaged momentum over the time step Δt . We follow the same particles that contribute to j^{LG} and time-average their velocities over a period of Δt :

$$j^{\Delta t}(\xi, t) = \frac{1}{\Delta t} \sum_n \int_{t-\Delta t}^t dt' v_n(t') \Delta_\xi [x_n(t)] \quad (20)$$

$$= \sum_n \frac{x_n(t) - x_n(t - \Delta t)}{\Delta t} \Delta_\xi [x_n(t)]. \quad (21)$$

This is a measure that shares the time step dependence with j^{LG} and at the same time is a measure that only depends on the MD data for the lattice cell. In that sense it is an intermediate measure. For Δt much shorter than the mean free time of the particles it should agree with j . We also examined the correlation between this measure of the momentum and the fundamental lattice gas momentum in Fig. 1. Comparing this measure $j^{\Delta t}$ to the fundamental momentum j we see that for the short time of $\Delta t = 0.366$ the two measures are indeed highly correlated. But for larger values of Δt the variance of $j^{\Delta t}$ becomes smaller than the variance of j , and at the same time the scatter increases.

When we compare $j^{\Delta t}$ to j^{LG} we see that for short times the behavior is essentially the same as for j and j^{LG} . For larger time steps Δt the $j^{\Delta t}$ is showing a narrowing of distribution which approaches that of j^{LG} . At the same time it can be seen in Fig. 1 that the correlation between j^{LG} and $j^{\Delta t}$ increases with larger Δt and the scatter decreases. It is hard to quantify this effect from a scatter plot, so instead we define a measure for the correlation.

We define a measure for the correlation of two quantities that allows for a relative scaling of the quantities by

$$C_{j^a, j^b}(\Delta t) = \frac{1}{2XT} \sum_\xi \sum_t \left[\frac{j^a(\xi, t)}{\sigma_{j^a}} - \frac{j^b(\xi, t)}{\sigma_{j^b}} \right]^2, \quad (22)$$

where X is the number of lattice sites and T is the number of time-steps we are averaging over. The variance σ_j are defined through

$$\sigma_j = \sqrt{\frac{1}{XT} \sum_\xi \sum_t [j(\xi, t) - \rho^{\text{eq}} u]^2}, \quad (23)$$

where $\rho^{\text{eq}} u$ is the average momentum per lattice cell of Eq. (18). For our simulations this is set to zero for simplicity. The measure C_{j^a, j^b} is zero when the two different measures j^a and j^b of momentum are completely correlated (i.e., identical up to a scaling factor) and will take on a value of one when they are completely uncorrelated. Note that this measure does take into account that even if the overall scale of the momentum, as given by the spread of the distribution, differs, the momenta could in principle still be strongly correlated.

The results of measuring these C_{j^a, j^b} functions are shown in Fig. 2. As we observed in our discussion of Fig. 1 there is close agreement between the fundamental definition of momentum $j(x, t)$ and the time-averaged momentum $j^{\Delta t}$ for small time intervals Δt . For larger time steps, this correlation begins to weaken.

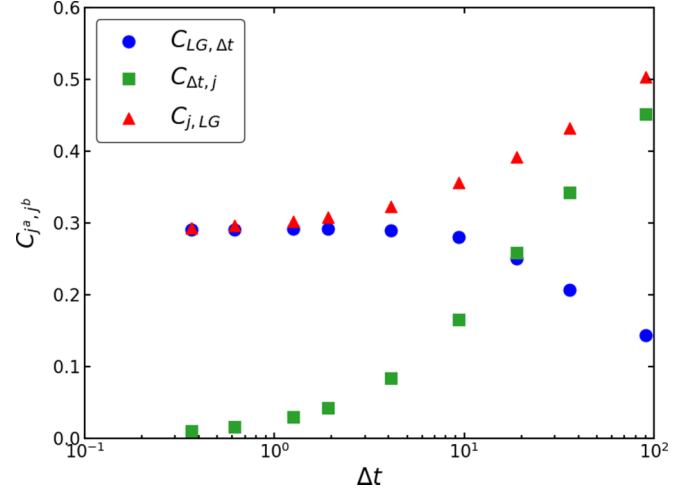


FIG. 2. Correlators of Eq. (22) for the three combinations of the three definitions of momentum considered in this paper. They are shown as a function of the time-step Δt .

We also observe that the correlation between the averaged momentum $j^{\Delta t}$ and the lattice gas momentum j^{LG} does indeed increase with an increasing time-step Δt as we surmised from the inspection of Fig. 1. We hypothesize that this correlation between $j^{\Delta t}$ and j^{LG} will continue to increase. Without being able to give a full proof here, we speculate that at larger coarse-graining the time-averaged velocities that enter both measures become more and more correlated, as was shown in an earlier paper [30]. As coarsening increases, fluctuations become less important and the observed time-averaged velocities will vary less within one lattice cell, leading to agreement between the two measures. Note, however, that this is a subtle effect of time-correlations, and coarse-graining alone is not sufficient, as can be seen in the deterioration of the correlations with the fundamental momentum j .

In the above discussion we examined the correlation of the different definitions of momenta normalized by their mean-squared displacements. But we have not considered the mean-squared displacements themselves. We show those second moments of the momenta, normalized by the average number of particles per cell, in Fig. 3 as a function of the time-step Δt . The most important feature to notice is that the second moment of the lattice gas diverges for small time steps from the results for the instantaneous (and the time-averaged) momentum. The observation that coarse-graining can lead to an increase as well as a decrease in fluctuations is somewhat unexpected and requires some careful analysis.

In the next part of this paper we will consider the distributions of momentum for the three different measures we defined, which can be achieved analytically in the limit of a small time-step. This will elucidate the curious result of the different fluctuation amplitudes for the lattice gas and instantaneous momenta.

IV. DISTRIBUTIONS OF THE MOMENTA

We observed an increase in the fluctuation for the lattice gas definition of momentum. We will now examine if we can understand these findings quantitatively and how they relate to

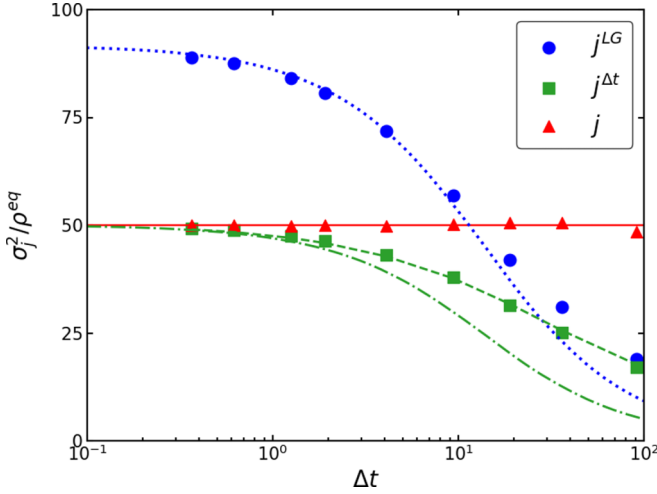


FIG. 3. Second moments of the three definitions of momentum from measurement (symbols) compared to theoretical predictions. The red triangles and the solid line correspond to the measurement of the current j and the ideal gas prediction of Eq. (33). The displacement momentum $j^{\Delta t}$ is shown as green squares and the ideal gas prediction of Eq. (42) is shown as a green dot-dashed line. The improved prediction including correlations of Eq. (51) is shown as a dashed line, and agrees well with the measurements. The lattice gas momentum j^{LG} is shown as blue circles, and the ideal gas prediction of Eq. (70) is shown as a blue dotted line.

previous predictions. First let us stress again that an ensemble average of the momentum (which would be free of fluctuations) does agree for all three definitions of the momentum. So we are interested here in the fluctuating component of the momentum.

A. Instantaneous momentum

For the lattice momentum measure j the situation is already rather interesting. We can calculate the momentum distribution as

$$P^j(j) = \int dx_1 dv_1 \cdots dx_N dv_N P^N(x_1, v_1, \cdots, x_N, v_N) \times \delta\left(j - \sum_{n=1}^N v_n \Delta_\xi(x_n)\right). \quad (24)$$

To obtain the average we need the N -particle distribution function in phase space in equilibrium. We assume here that the mean velocity is u . We define the average number of particles per lattice cell as

$$\rho^{eq} = \frac{N(\Delta x)^d}{L^d}, \quad (25)$$

which is identical to the definition of Eq. (18). Since we are considering a system in equilibrium here all particles have uncorrelated velocities distributed according to the Maxwell Boltzmann distribution

$$P^{MB}(v) = \frac{1}{(2\pi k_B T)^{d/2}} \exp\left(-\frac{(v-u)^2}{2k_B T}\right), \quad (26)$$

k_B is Boltzmann's constant and T is the temperature. For simplicity we will assume $u = 0$ below. The extension to nonzero

u is straightforward but makes the expressions below longer. If we further assume that the particles are dilute enough so that they resemble an ideal gas, then the N -particle distribution function is simply given by

$$P^N(x_1, v_1, \cdots, x_N, v_N, t) = \prod_{n=1}^N \frac{1}{V} P^{MB}(v_n); \quad (27)$$

otherwise, volume exclusion has to be taken into account. In this case the number of particles in a cell will be Poisson distributed and we get

$$P^j(j) = \exp(-\rho^{eq}) \left[\delta(j) + \sum_{n=1}^{\infty} \frac{(\rho^{eq})^n}{n!} \exp\left(-\frac{j^2}{2nk_B T}\right) \right], \quad (28)$$

where the appearance of a Dirac δ function represents the finite fraction of lattice cells without particles that contain a momentum of zero. This distribution function is an unusual combination of a discrete set of Gaussians and one δ function that can be understood as the limit of a Gaussian with zero width. It was the discovery of this unusual distribution function that inspired its application in a quite different context in a recent paper by Pachalieva [31].

Interestingly the second moment of this distribution can be evaluated directly, without requiring the assumption in Eq. (27) of a dilute gas. We get

$$\langle j(\xi, t)^2 \rangle \quad (29)$$

$$= \left\langle \left(\sum_n v_n(t) \Delta_\xi(x_n(t)) \right)^2 \right\rangle \quad (30)$$

$$= \int dx_1 dv_1 \cdots dx_N dv_N P^N(x_1, v_1, \cdots, x_N, v_N) \times \sum_{n=1}^N \sum_{m=1}^N v_n v_m \Delta_\xi(x_n) \Delta_\xi(x_m) \quad (31)$$

$$= N \frac{\Delta x^d}{V} \int dv_1 (v_1)^2 P^{MB}(v_1) \quad (32)$$

$$= d \rho^{eq} k_B T, \quad (33)$$

where we have used that the expectation value of a single velocity term is zero by symmetry and that the velocities of any two particles are uncorrelated in equilibrium, leaving on the one-particle contribution above. This is a result well known from kinetic theory, and our simulation results are in very good agreement with this theory, as shown in Fig. 3.

B. Displacement momentum

For the momentum defined from the particle displacement the situation is a little more complicated. Analogous to the previous case we need to calculate

$$P^{\Delta t}(j) = \int dx_1 dv_1 \cdots dx_N dv_N P^{N,\delta}(x_1, \delta x_1, \cdots, x_N, \delta x_N) \times \delta\left(j - \sum_{n=1}^N \frac{\delta x_n}{\Delta t} \Delta_\xi(x_n)\right), \quad (34)$$

but, as was emphasized by Pachaliev *et al.* [31], little is known about the N -particle displacement distribution function. For short time-steps Δt it is reasonable to assume that in equilibrium this distribution function will also factorize, but because the time-evolution introduces correlations, this ceases to be valid for larger time-steps. For dilute systems, the buildup of these correlations is less severe [30], so the assumption of a factorizing distribution function is not immediately invalid.

As a second approximation we will assume here that the factorizing single particle displacement distribution function can be approximated by a Gaussian. We know that this is only approximately true [31], but it will serve here for a rough approximation. We therefore assume

$$P^{\Delta t}(\delta x) \approx \frac{1}{(2\pi \langle \delta x^2 \rangle)^{d/2}} \exp\left(-\frac{(\delta x - u\Delta t)^2}{2\langle \delta x^2 \rangle}\right), \quad (35)$$

where the mean-squared displacement $\langle \delta x^2 \rangle$ is to be obtained from the numerical simulations as usual [25]. We also assume that the particles are uniformly distributed.

With this assumption we can calculate an approximate second moment for the time-averaged momentum:

$$\langle j^{\Delta t}(\xi, t)^2 \rangle \quad (36)$$

$$= \left\langle \left(\sum_n \frac{x_n(t) - x_n(t - \Delta t)}{\Delta t} \Delta_\xi(x_n(t)) \right)^2 \right\rangle \quad (37)$$

$$= \int dx_1 d\delta x_1 \cdots dx_N d\delta x_N P^N(x_1, \delta x_1, \dots, x_N, \delta x_N) \times \sum_{n=1}^N \sum_{m=1}^N \delta x_n \delta x_m \Delta_\xi(x_n) \Delta_\xi(x_m) \quad (38)$$

$$= N(N-1) \int dx_1 d\delta x_1 dx_2 d\delta x_2 P^{2,\Delta t}(x_1, \delta x_1, x_2, \delta x_2) \times \frac{\delta x_1 \delta x_2}{(\Delta t)^2} \Delta_\xi(x_1) \Delta_\xi(x_2) + N \int dx_1 d\delta x_1 \left(\frac{\delta x_1}{\Delta t} \right)^2 P^{\Delta t}(x_1, \delta x_1). \quad (39)$$

The last term can be easily evaluated as

$$N \int dx_1 d\delta x_1 \left(\frac{\delta x_1}{\Delta t} \right)^2 P^{\Delta t}(x_1, \delta x_1) \Delta_\xi(x_1) \quad (40)$$

$$= N \frac{\Delta x^d}{L^d} \int d\delta x_1 \left(\frac{\delta x_1}{\Delta t} \right)^2 P^{\Delta t}(\delta x_1) \quad (41)$$

$$= \rho^{\text{eq}} \frac{\langle \delta x^2 \rangle}{(\Delta t)^2}. \quad (42)$$

The first term contains a two-particle probability distribution that has been approximated previously [30] by

$$P^{2,\Delta t}(x_1, \delta x_1, x_2, \delta x_2) \approx \frac{1}{L^{2d}} g(r) \exp\left(-\frac{(\delta x_1 + \delta x_2)^2}{4\sigma_+^2(r)}\right) \exp\left(-\frac{(\delta x_1 - \delta x_2)^2}{4\sigma_-^2(r)}\right), \quad (43)$$

where $r = |x_1 - x_2|$,

$$\sigma_\pm(r) = a\Delta x \sqrt{\frac{1 \pm \langle \delta x_1 \delta x_2 \rangle}{\langle \delta x_1 \delta x_1 \rangle}}, \quad (44)$$

and $g(r)$ is the radial distribution function. It is here approximated by [25]

$$g(r) = \frac{1}{2} \tanh\left(\frac{r - \zeta}{0.03}\right) + \frac{1}{2}, \quad (45)$$

and we use $\zeta = 0.75$. Two important properties of this two particle displacement distribution function is that

$$\int d\delta x_1 d\delta x_2 \delta x_1^2 P^{2,\Delta t}(x_1, \delta x_1, x_2, \delta x_2) = \frac{g(r)}{L^4} \langle \delta x^2 \rangle, \quad (46)$$

$$\int d\delta x_1 d\delta x_2 \delta x_1 \delta x_2 P^{2,\Delta t}(x_1, \delta x_1, x_2, \delta x_2) = \frac{g(r)}{L^4} \langle \delta x_1 \delta x_2 \rangle. \quad (47)$$

The correlation of displacements as a function of distance was found to be well approximated by

$$\langle \delta x_1 \delta x_2 \rangle(r) \approx \kappa \langle \delta x^2 \rangle \left(\frac{\rho}{\sqrt{\langle \delta x^2 \rangle}} \right)^{1/2} \exp\left(-\frac{r}{\xi \sqrt{\langle \delta x^2 \rangle}}\right) \quad (48)$$

$$= \kappa a^{-1/2} \langle \delta x^2 \rangle \left(\frac{\rho}{\Delta x} \right)^{1/2} \exp\left(-\frac{r}{\xi a \Delta x}\right), \quad (49)$$

where ξ varied only very slightly with density from 1 for low densities to 1.25 for the highest densities tested. For the last step we used Eq. (9). We find that we get good agreement for $\kappa = 0.38$ and we hope to perform more thorough analysis of the origin of these correlation effects in a future study. We here take $\xi = 1$ since our density is closer to the low densities considered in [30]. We can now evaluate (making the approximation $N - 1 \approx N$)

$$N^2 \int dx_1 d\delta x_1 dx_2 d\delta x_2 P^{2,\Delta t}(x_1, \delta x_1, x_2, \delta x_2) \times \frac{\delta x_1 \delta x_2}{(\Delta t)^2} \Delta_\xi(x_1) \Delta_\xi(x_2) = \left(\frac{N}{L^2} \right)^2 \int dx_1 dx_2 \frac{\langle \delta x_1 \delta x_2 \rangle(r)}{(\Delta t)^2} \Delta_\xi(x_1) \Delta_\xi(x_2) = \kappa a^{-1/2} \left(\frac{\rho^{\text{eq}}}{\Delta x} \right)^{5/2} \langle \delta_1 \delta_1 \rangle \times \int dx_1 dx_2 \frac{g(r)}{(\Delta x)^4} \exp\left(-\frac{r}{\xi a \Delta x}\right) \Delta_\xi(x_1) \Delta_\xi(x_2). \quad (50)$$

This last integral can only be performed numerically, but we define

$$C(\Delta x) = \int dx_1 dx_2 \frac{g(r)}{(\Delta x)^4} \exp\left(-\frac{\sqrt{6}r}{\xi \Delta x}\right) \Delta_\xi(x_1) \Delta_\xi(x_2). \quad (51)$$

We find that to good approximation

$$C(\Delta x) \approx 0.333 \quad (52)$$

for $\Delta x > 20$ and goes to zero at $\Delta x \rightarrow \zeta$. The full form is shown in the supplemental material [32]. With this we obtain

$$\langle j^{\Delta t}(\xi, t)^2 \rangle = \rho^{\text{eq}} \frac{\langle \delta x^2 \rangle}{(\Delta t)^2} \left(1 + \kappa a^{-1/2} \left(\frac{\rho^{\text{eq}}}{\Delta x} \right)^{3/2} C(\Delta x) \right), \quad (53)$$

which is in excellent agreement with the data, as can be seen in Fig. 3.

C. Lattice gas momentum

Let us now put our attention on the lattice gas momentum. It was first claimed by Adhikari *et al.* [5] and later by Dünweg *et al.* [6] that the occupation numbers n_i should be Poisson distributed as long as we are considering an ideal gas. This argument was based on the arguments presented in Landau and Lifshitz [33]. A more general derivation of the distribution was given in our previous publication [30], where it was shown that in general the distribution of the n_i depends on the N -particle distribution function. This is a slight simplification from the derivation of Eq. (19), where a finite system leading to a multinomial distribution was considered. For that derivation, however, it was assumed that the only values for the velocity in any one direction would be zero or $\pm \Delta x / \Delta t$. The derivation using the assumption of Poisson distributed occupation numbers is simpler than generalizing the previous derivation.

In the special case that this distribution function factorizes, as was assumed in the previous section for the analytical calculation of the momentum distribution for the $j^{\Delta t}$ momentum measure, the occupation numbers n_i are indeed Poisson distributed. With this approximation Parsa *et al.* [30] obtained

$$P(n_i) = \exp(-f_i^{\text{eq}}) \frac{(f_i^{\text{eq}})^{n_i}}{n_i!}, \quad (54)$$

where the equilibrium distribution are given by Eq. (8). A fully analytical expression for f_i^{eq} can be obtained analytically [25,34,35] by solving

$$f_i^{\text{eq}} = \int dx \int d\delta x P^{\Delta t}(\delta x) \Delta_\xi(x) \Delta_{\xi-c_i}(x - \delta x), \quad (55)$$

where $\Delta_\xi(x)$ was defined in Eq. (2). While Mathematica is able to obtain an explicit expression for the solution, it is too lengthy to reproduce here. It can be found in the Mathematica notebook in the Supplemental Material [32].

Of interest here are the first three moments of the equilibrium distribution. The zeroth and first velocity moments are given by mass and momentum conservation, as was shown by Parsa *et al.* [25]. The second velocity moment, however, is more interesting. It was previously evaluated for $u = 0$ in the same publication, but here we also evaluate it for general u . The moments are given by

$$\sum_i f_i^{\text{eq}} = \rho^{\text{eq}}, \quad (56)$$

$$\sum_i v_{i\alpha} f_i^{\text{eq}} = \rho^{\text{eq}} u_\alpha, \quad (57)$$

$$\sum_i v_{i\alpha} v_{i\beta} f_i^{\text{eq}} = \rho u_\alpha u_\beta + \delta_{\alpha\beta} \theta, \quad (58)$$

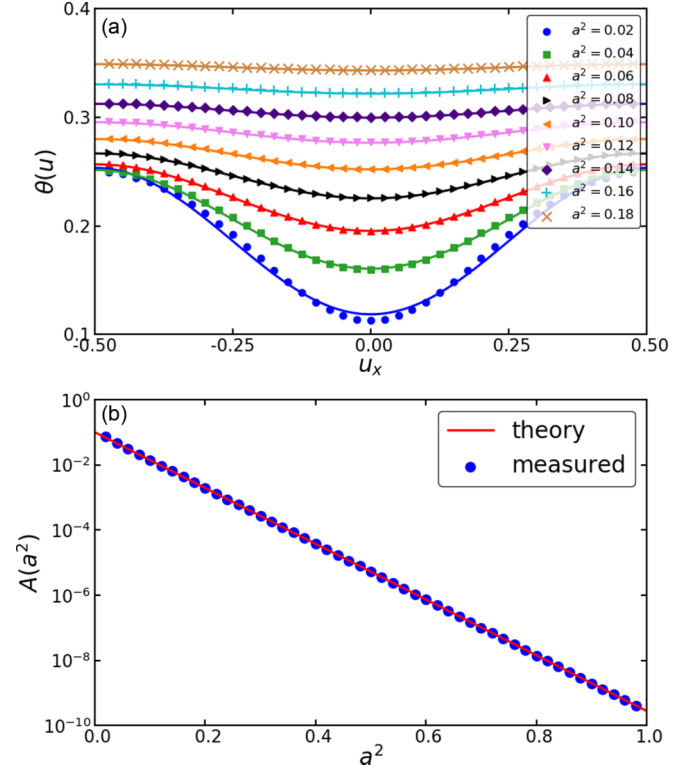


FIG. 4. θ defined in Eq. (58) as function of mean velocity for different a^2 is shown in panel (a) and the measured amplitude $A(a^2)$ is shown in panel (b). Both are compared to the numerical fit of Eq. (67).

where $\theta(\Delta t, \Delta x)$ is defined by Eq. (58). It approaches $a^2 + 1/6$, with a^2 defined in Eq. (9), which was previously shown in Fig. 10 of Ref. [25]. What is new here is that we were able to show that this result holds all values of u . In the context of the research for this paper we discovered that while the discussion in the paper by Parsa *et al.* focused on the case $u = 0$, the dependence on u for different θ is actually fascinating. While lattice Boltzmann approaches demand that θ is a constant, this requirement is not consistent with the requirement of a positive distribution f_i^{eq} for small values of θ .

Numerical evidence shows that we can approximate

$$\theta(u_x, u_y \equiv 0) = \left[\left(a^2 + \frac{1}{6} \right) - A(a^2) \cos(2\pi u_x) \right], \quad (59)$$

with

$$A(a^2) = 0.1 \exp(-19.7a^2), \quad (60)$$

where the numerical values were found by numerical fitting, as shown in Fig. 4. This shows that while the lattice gas expression for the second moment cannot be strictly Galilean invariant, it exponentially approaches a Galilean invariant value for larger a^2 .

These results allow us to make an analytical prediction for lattice gas momentum fluctuations for a dilute system. The probability of observing a momentum of j for a lattice gas is given by a combination of Poisson distributed random

numbers:

$$P^{\text{LG}}(j) = \sum_{n_1=0}^N \cdots \sum_{n_I=0}^N P(\{n_i\}) \delta\left(j - \sum_i n_i c_i\right), \quad (61)$$

where $\delta()$ is the δ function and I is the number of discrete lattice velocities. To evaluate this, it makes sense to first combine all the contributions with a positive velocity $c_{ix} > 0$. For this purpose let us define a partial velocity set c_{ix}^+ with V^+ elements, which contains all velocities with a positive x component. We then get for the probability of having j^+ particles with positive x lattice gas displacement

$$\begin{aligned} P(j^+) &= \sum_{n_1^+=0}^{\widehat{j}^+} \cdots \sum_{n_{V^+}^+=0}^{\widehat{j}^+} \prod_{i=1}^{V^+} e^{-f_i^{\text{eq}}} \frac{(f_i^{\text{eq}})^{n_i^+}}{n_i^+!} \delta\left(\sum_i n_i^+ c_{ix}^+ - j^+\right) \\ &= e^{-\sum_{i=1}^{V^+} f_i^+} \frac{(\sum_i f_i^+)^{\widehat{j}^+}}{\widehat{j}^+!}, \end{aligned} \quad (62)$$

where we introduced an integer momentum as $\widehat{j}^+ = j^+ \Delta t / \Delta x$. Similarly, we get

$$P(j^-) = e^{-\sum_{i=1}^{V^-} f_i^-} \frac{(\sum_i f_i^-)^{\widehat{j}^-}}{\widehat{j}^-!}. \quad (63)$$

The probability distribution for the full nondimensional momentum $\widehat{j} = j \Delta t / \Delta x$ is then given by

$$\begin{aligned} P^{\text{LG}}(\widehat{j}) &= \sum_{\widehat{j}^+=0}^{\infty} \sum_{\widehat{j}^-=0}^{\infty} e^{-(f^++f^-)} \frac{(f^+)^{\widehat{j}^+}}{\widehat{j}^+!} \frac{(f^-)^{\widehat{j}^-}}{\widehat{j}^-!} \delta_{(\widehat{j}^+-\widehat{j}^-), \widehat{j}} \\ &= e^{-(f^++f^-)} \sum_{\widehat{j}^+=\max(0, \widehat{j})}^{\infty} \frac{(f^+)^{\widehat{j}^+}}{\widehat{j}^+!} \frac{(f^-)^{\widehat{j}^+-\widehat{j}}}{(\widehat{j}^+-\widehat{j})!} \\ &= e^{-(f^++f^-)} \left(\frac{f^+}{f^-}\right)^{\widehat{j}/2} I_{|\widehat{j}|}(2\sqrt{f^+f^-}), \end{aligned} \quad (64)$$

where $I_j()$ is the modified Bessel function of the first kind. This result will be identical to Eq. (19) when $N_\xi \rightarrow \infty$, i.e., the system becomes infinite. Looking back at Eq. (57) and Eq. (58) we see that we can identify

$$(f^+ - f^-) \frac{\Delta x}{\Delta t} = \rho u_x, \quad (65)$$

$$(f^+ + f^-) \frac{\Delta x^2}{\Delta t^2} = \rho u_x^2 + \rho \theta. \quad (66)$$

So we can write the probability distribution for the current in terms of the equilibrium properties as

$$\begin{aligned} P^{\text{LG}}(\widehat{j}) &= e^{-(\rho u_x^2 + \rho \theta)} \left(\frac{u_x + u_x^2 + \theta}{-u_x + u_x^2 + \theta} \right)^{\widehat{j}/2} \\ &\quad \times I_{|\widehat{j}|} \sqrt{\rho(u_x^2 + \theta)^2 - \rho^2 u_x^2}. \end{aligned} \quad (67)$$

With this we obtain in MD units

$$\sum_j P^{\text{LG}}(j) j = \rho u, \quad (68)$$

$$\sum_j P^{\text{LG}}(j) j^2 = \rho u_x^2 + \rho \theta, \quad (69)$$

as should be expected for consistency with Eqs. (56)–(58). In particular for the case $u = 0$ we predict

$$\begin{aligned} \langle j^{\text{LG}}(\xi, t)^2 \rangle &= \rho^{\text{eq}} \theta \\ &\approx \rho^{\text{eq}} \left(\frac{\langle \delta x^2 \rangle}{\Delta x^2} + 1/6 \right) \frac{\Delta x^2}{\Delta t^2} \\ &= \rho^{\text{eq}} \left(\frac{\langle \delta x^2 \rangle}{\Delta t^2} + \frac{\Delta x^2}{6 \Delta t^2} \right). \end{aligned} \quad (70)$$

When comparing this to the results for $P^{\Delta t}$ of Eq. (42) we see that the first terms are identical, but there is a second term for the Lattice Gas. For the case of $a^2 = \langle \delta x^2 \rangle / \Delta x^2 = 2/11$ considered in this paper both terms are of equal magnitude, and we predict that the noise amplitude is a little less than twice as large for the lattice gas current than for the current defined by displacements.

V. DISCUSSION

In this article we have investigated coarse-grained descriptions of momentum fluctuations. Of particular interest to us were lattice gas momentum fluctuations. We were able to show that in a lattice gas coarse-graining that maps a molecular dynamics simulation onto a lattice gas, the momentum fluctuations are significantly enhanced. This is in contrast to density fluctuations, that have been carefully studied, and that agree extremely well with experimental results [16]. A comparison of the predictions for the current fluctuations with the actually measured current fluctuations for different Δt was shown in Fig. 3. The fundamental definition of the momentum j has fluctuations that are independent of Δt . The time-averaged current $j^{\Delta t}$ fluctuations agree with the fundamental current for small Δt , where the approximation $v = \delta x / \Delta t$ holds but then starts to be reduced. The actually measured fluctuations of this current, however, are significantly less reduced than the ideal gas theory of Eq. (42) would predict. Correlations between particle displacements have to be taken into account to understand this observation, as has been foreshadowed in [30]. Taking into account the correlations of particles displacements in Eq. (53) is possible and allows us to explain the observed fluctuations.

The fluctuations for the lattice gas current j^{LG} fail to converge with the fundamental current fluctuations, even for small Δt . They do, however, agree well with the experimentally measured lattice gas current fluctuations. For large Δt the measured displacement and lattice gas currents start to converge.

The lack of convergence of the fluctuations of lattice gas momentum with the other two definitions of momentum for small time step raises the question what the nature of the remaining significant difference is. Initially it appeared to us that the most likely explanation was that the existence of a lattice can introduce effects at the scale of the lattice size,

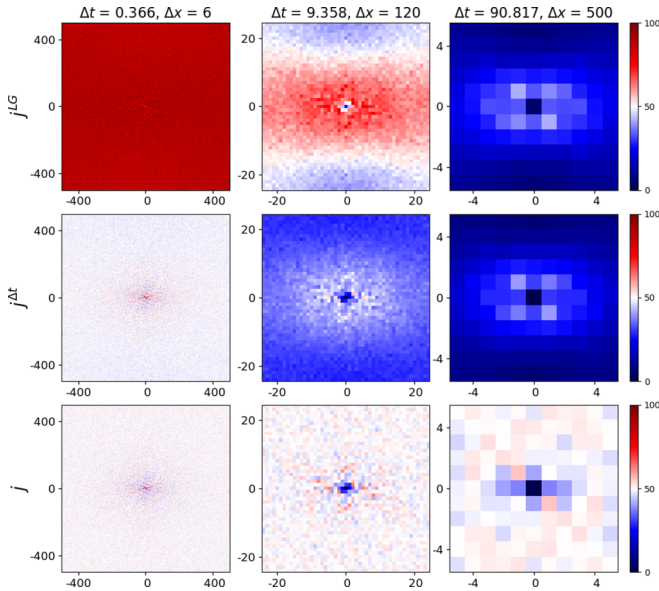


FIG. 5. Fourier transforms $\langle j^a(k)j^a(-k) \rangle$ for three different current definitions $j^a = \{j, j^{\Delta t}, j^{\text{LG}}\}$ considered in this paper for three different time-steps Δt .

whereas we expected long wave-length fluctuations, which evolve much slower and are therefore less affected by time-averaging, to coincide. This would also be consistent with the expectation that in the hydrodynamic limit all currents should agree. We therefore looked at the Fourier transforms of the current fluctuations for all three currents at three different levels of coarse graining. The results are shown in Fig. 5. As expected for the dilute system under consideration, the fluctuations for the x component of the current j are always flat. The Fourier plot for the time-averaged current $j_x^{\Delta t}$ is identical for small Δt , but for larger Δt the current diminishes for fast modes corresponding to short wavelength, and this effect is clearly visible in the graph. It is also obvious that current in the orthogonal y -direction decays more quickly whereas the value for slowly evolving large wavelength (small k) remains essentially unaffected by the time-averaging.

Now the Fourier transform of the lattice gas current is also k -independent, but at the much higher fluctuation amplitudes as predicted by Eq. (70). This implies that the lattice gas discretization changes the fluctuation amplitude of the noise-component of the current even for very large wavelength, while not affecting the ensemble averaged current. This result was unexpected, since we anticipated that the agreement of the three-momentum measures in the thermodynamic limit would imply that they should also agree in the large wavelength limit.

For the larger time-step of $\Delta t = 9.358$ we saw in Fig. 3 that the total fluctuation amplitude still tracks the analytically predicted one very closely. Here we see, however, that the Fourier spectrum is no longer flat but instead decays, particularly in the orthogonal direction. At the even larger time-step of $\Delta t = 90.817$ we saw in Fig. 3 that the analytical prediction and the measured fluctuations no longer agree. However, we also saw that the overall fluctuations of $j^{\Delta t}$ and j^{LG} converged. Here we now observe that even the full Fourier representations of the two measures agree.

In conclusion, we have discussed three definitions of momentum to examine the effect of different coarse-graining procedures on the definition of the fundamental conserved quantity of momentum. We found that different coarse-grained definitions of the momentum can disagree for the fluctuating components, even in the hydrodynamic limit, while ensemble averages of the momenta fully agree. This result is in full agreement with our analytical predictions. We saw that for short coarse-graining times Δt the lattice gas does obey the predictions for fluctuations underlying the work of Adhikari *et al.* [5] as well as later research [6,22,23,36], but the momentum fluctuations are about twice as large as the fluctuations of the fundamental definition of momentum of a lattice cell.

Another result that requires further investigation is that the lattice gas momentum starts to converge towards another fundamental time-averaged definition of momentum for larger Δt , and in this limit numerical evidence suggests that the momentum fluctuations for large wavelength now agree with the fluctuations corresponding the fundamental definition of momentum.

-
- [1] A. N. Gorban, Basic types of coarse-graining, in *Model Reduction and Coarse-Graining Approaches for Multiscale Phenomena*, edited by A. N. Gorban, I. G. Kevrekidis, C. Theodoropoulos, N. K. Kazantzis, and H. C. Öttinger (Springer, Berlin, 2006), pp. 117–176.
- [2] U. Frisch, B. Hasslacher, and Y. Pomeau, Lattice-Gas Automata for the Navier-Stokes Equation, *Phys. Rev. Lett.* **56**, 1505 (1986).
- [3] J. P. Boon and S. Yip, *Molecular Hydrodynamics* (Courier Corporation, Mineola, NY, 1991).
- [4] A. J. C. Ladd, Short-Time Motion of Colloidal Particles: Numerical Simulation via a Fluctuating Lattice-Boltzmann Equation, *Phys. Rev. Lett.* **70**, 1339 (1993).
- [5] R. Adhikari, K. Stratford, M. Cates, and A. Wagner, Fluctuating lattice Boltzmann, *Europhys. Lett.* **71**, 473 (2005).
- [6] B. Dünweg, U. D. Schiller, and A. J. C. Ladd, Statistical mechanics of the fluctuating lattice Boltzmann equation, *Phys. Rev. E* **76**, 036704 (2007).
- [7] P. Grosfils, J.-P. Boon, and P. Lallemand, Spontaneous Fluctuation Correlations in Thermal Lattice-Gas Automata, *Phys. Rev. Lett.* **68**, 1077 (1992).
- [8] P. Hoogerbrugge and J. Koelman, Simulating microscopic hydrodynamic phenomena with dissipative particle dynamics, *Europhys. Lett.* **19**, 155 (1992).
- [9] P. Espanol and P. Warren, Statistical mechanics of dissipative particle dynamics, *Europhys. Lett.* **30**, 191 (1995).
- [10] T. Ihle and D. M. Kroll, Stochastic rotation dynamics: A Galilean-invariant mesoscopic model for fluid flow, *Phys. Rev. E* **63**, 020201(R) (2001).

- [11] T. Ihle and D. M. Kroll, Stochastic rotation dynamics. I. Formalism, Galilean invariance, and Green-Kubo relations, *Phys. Rev. E* **67**, 066705 (2003).
- [12] E. Tüzel, M. Strauss, T. Ihle, and D. M. Kroll, Transport coefficients for stochastic rotation dynamics in three dimensions, *Phys. Rev. E* **68**, 036701 (2003).
- [13] S. Wolfram, Cellular automaton fluids 1: Basic theory, *J. Stat. Phys.* **45**, 471 (1986).
- [14] A. J. C. Ladd, M. E. Colvin, and D. Frenkel, Application of Lattice-Gas Cellular Automata to the Brownian Motion of Solids in Suspension, *Phys. Rev. Lett.* **60**, 975 (1988).
- [15] A. J. Ladd and D. Frenkel, Dissipative hydrodynamic interactions via lattice-gas cellular automata, *Phys. Fluids A* **2**, 1921 (1990).
- [16] J.-P. Rivet and J.-P. Boon, *Lattice Gas Hydrodynamics*, Vol. 11 (Cambridge University Press, Cambridge, UK, 2005).
- [17] D. Frenkel and M. H. Ernst, Simulation of Diffusion in a Two-Dimensional Lattice-Gas Cellular Automaton: A Test of Mode-Coupling Theory, *Phys. Rev. Lett.* **63**, 2165 (1989).
- [18] F. J. Higuera and J. Jiménez, Boltzmann approach to lattice gas simulations, *Europhys. Lett.* **9**, 663 (1989).
- [19] F. Higuera, S. Succi, and R. Benzi, Lattice gas dynamics with enhanced collisions, *Europhys. Lett.* **9**, 345 (1989).
- [20] Y.-H. Qian, D. d’Humières, and P. Lallemand, Lattice BGK models for Navier-Stokes equation, *Europhys. Lett.* **17**, 479 (1992).
- [21] A. J. Ladd, Numerical simulations of particulate suspensions via a discretized Boltzmann equation. Part I. Theoretical foundation, *J. Fluid Mech.* **271**, 285 (1994).
- [22] G. Kaehler and A. J. Wagner, Fluctuating ideal-gas lattice Boltzmann method with fluctuation dissipation theorem for nonvanishing velocities, *Phys. Rev. E* **87**, 063310 (2013).
- [23] T. Blommel and A. J. Wagner, Integer lattice gas with Monte Carlo collision operator recovers the lattice Boltzmann method with poisson-distributed fluctuations, *Phys. Rev. E* **97**, 023310 (2018).
- [24] S. Ansumali, I. V. Karlin, and H. C. Öttinger, Minimal entropic kinetic models for hydrodynamics, *Europhys. Lett.* **63**, 798 (2003).
- [25] M. R. Parsa and A. J. Wagner, Lattice gas with molecular dynamics collision operator, *Phys. Rev. E* **96**, 013314 (2017).
- [26] P. Español, M. Serrano, and I. Zuñiga, Coarse-graining of a fluid and its relation with dissipative particle dynamics and smoothed particle dynamic, *Int. J. Mod. Phys. C* **8**, 899 (1997).
- [27] R. E. Rudd and J. Q. Broughton, Coarse-grained molecular dynamics and the atomic limit of finite elements, *Phys. Rev. B* **58**, R5893 (1998).
- [28] S. Plimpton, Fast parallel algorithms for short-range molecular dynamics, *J. Comput. Phys.* **117**, 1 (1995).
- [29] W. F. Godoy, N. Podhorszki, R. Wang, C. Atkins, G. Eisenhauer, J. Gu, P. Davis, J. Choi, K. Germaschewski, K. Huck *et al.*, Adios 2: The adaptable input output system. A framework for high-performance data management, *SoftwareX* **12**, 100561 (2020).
- [30] M. R. Parsa and A. J. Wagner, Large Fluctuations in Non-ideal Coarse-Grained Systems, *Phys. Rev. Lett.* **124**, 234501 (2020).
- [31] A. Pachalieva and A. J. Wagner, Non-Gaussian distribution of displacements for Lennard-Jones particles in equilibrium, *Phys. Rev. E* **102**, 053310 (2020).
- [32] See Supplemental Material at <http://link.aps.org/supplemental/10.1103/PhysRevE.104.015304> for a Mathematica notebook allowing readers to reproduce the calculations omitted in the article.
- [33] L. P. Pitaevskii, E. M. Lifshitz, and J. B. Sykes, *Physical Kinetics*, Vol. 10 (Pergamon, 1981), 1st ed.
- [34] M. R. Parsa, A. Pachalieva, and A. J. Wagner, Validity of the molecular-dynamics-lattice-gas global equilibrium distribution function, *Int. J. Mod. Phys. C* **30**, 1941007 (2019).
- [35] M. R. Parsa, Lattice gases with molecular dynamics collision operator, Ph.D. thesis, North Dakota State University, 2018.
- [36] A. J. Wagner and K. Strand, Fluctuating lattice Boltzmann method for the diffusion equation, *Phys. Rev. E* **94**, 033302 (2016).